

Supplementary Figure 1 (Fig. S1)

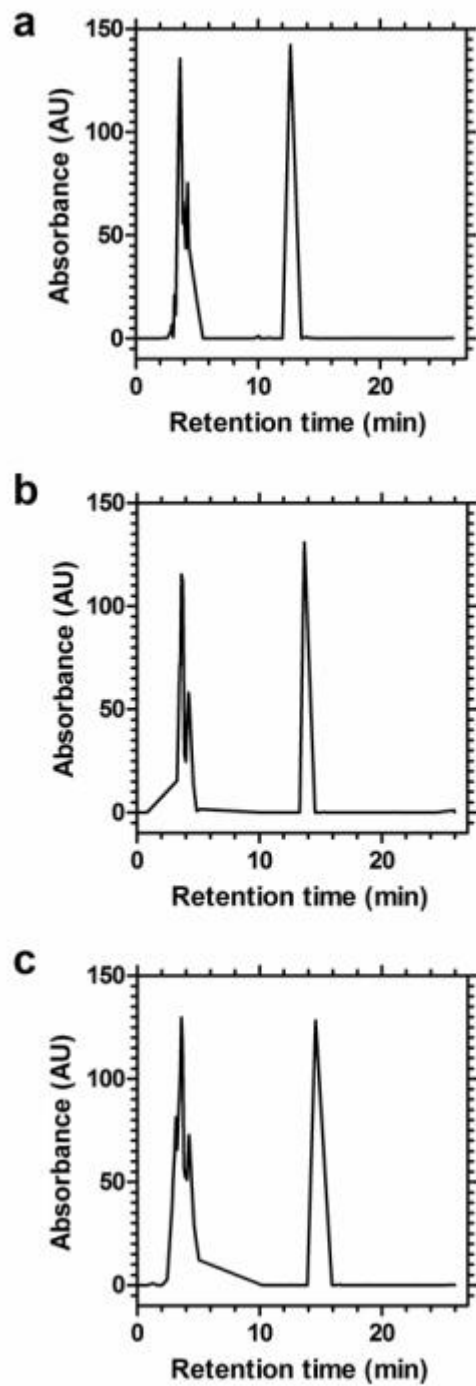


Fig. S1: HPLC traces of (a) dpA3 (b) dpV3 (c) dpI3. All synthesized conjugates were run on a C4 reverse phase semi prep column under a H₂O:ACN gradient. The chromatograms show that the synthesized conjugates are >95% pure. The peak at 1-2 mins is the system peak for methanol

Supplementary Table (Table. S1)

ELPA	Sequence	Expected Mass (Da)	Observed Mass (Da)
KA3	K(VPGAG) ₃	[M+H+]= 1290.4	[M+H+]= 1289.8
		[M+Na+]=1312.5	[M+Na+]= N.O
KI3	K(VPGIG) ₃	[M+H+]= 1416.7	[M+H+]= 1416.1
		[M+Na+]= 1438.	[M+Na+]= N.O.
KV3	K(VPGVG) ₃	[M+H+]= 1374.6	[M+H+]= 1375.1
		[M+Na+]= 1396.6	[M+Na+]= N.O.
dpA3	dp-K(VPGAG) ₃	[M+H+]= 1767.2	[M+H+]= 1766.7
		[M+Na+]= 1789.2	[M+Na+]= N.O.
dpI3	dp-K(VPGIG) ₃	[M+H+]= 1893.5	[M+H+]= 1892.9
		[M+Na+]= 1915.5	[M+Na+]= 1915.1
dpV3	dp-K(VPGVG) ₃	[M+H+]= 1849.6	[M+H+]= 1850.9
		[M+Na+]= 1871.6	[M+Na+]= N.O.

Table. S1: Physico-chemical characterization of ELPAs. The purified ELPAs were dissolved in HPLC grade methanol and run on a Thermo scientific LcQ-DECA ESI mass spectrometer. The observed mass confirms dipalmitoylation of the ELP sequence.

Supplementary Figure 2 (Fig. S2)

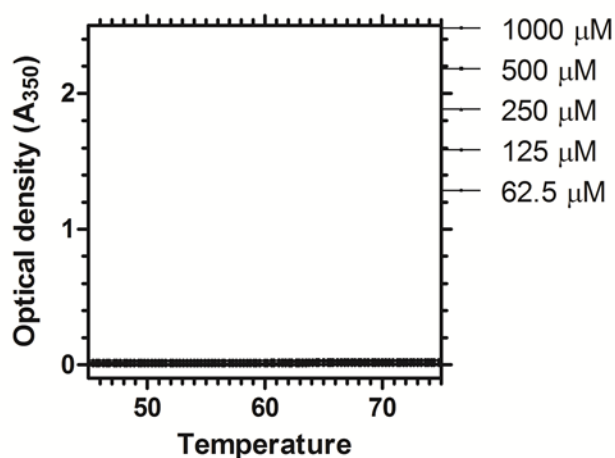


Fig. S2: KA3 does not exhibit phase transition behavior. Optical density measurements of KA3 were made at increasing temperatures. No transition behavior was observed below 80 °C.

Supplementary Figure 3 (Fig. S3)

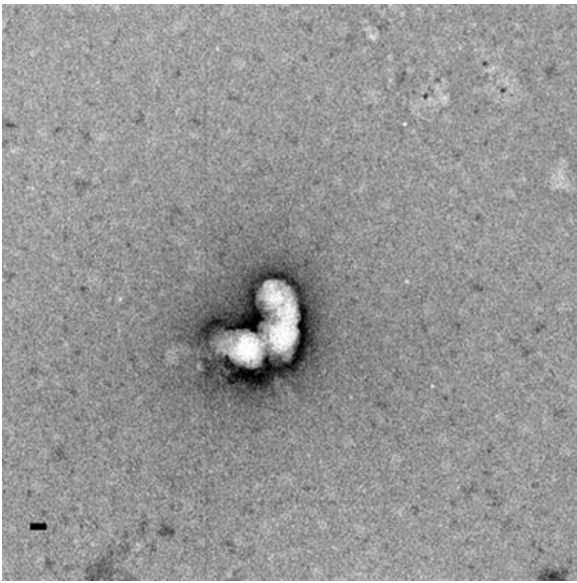


Fig. S3: KA3 does not assemble ordered structure. 1mM of unmodified KA3 was dried on a formvar carbon grid and imaged using negative staining transmission electron microscopy (uranyl acetate). TEM images of KA3 show aggregates with no ordered structure. Scale bar 50nm.

Supplementary Figure 4 (Fig. S4)

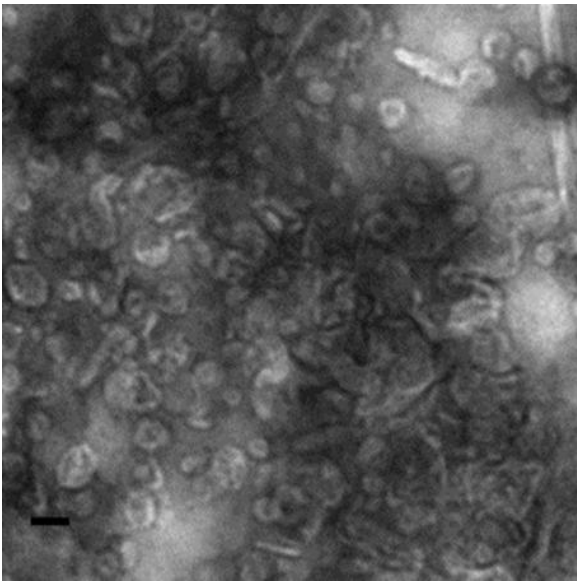


Fig. S4: High ratios of phospholipids eliminate fibril structures. A mixture of DOPE:dpA3 [9:1] was prepared using negative staining transmission electron microscopy (uranyl acetate). Instead of fibril structures, round structures were observed. Scale bar is 50nm.

Supplementary Figure 5 (Fig. S5)

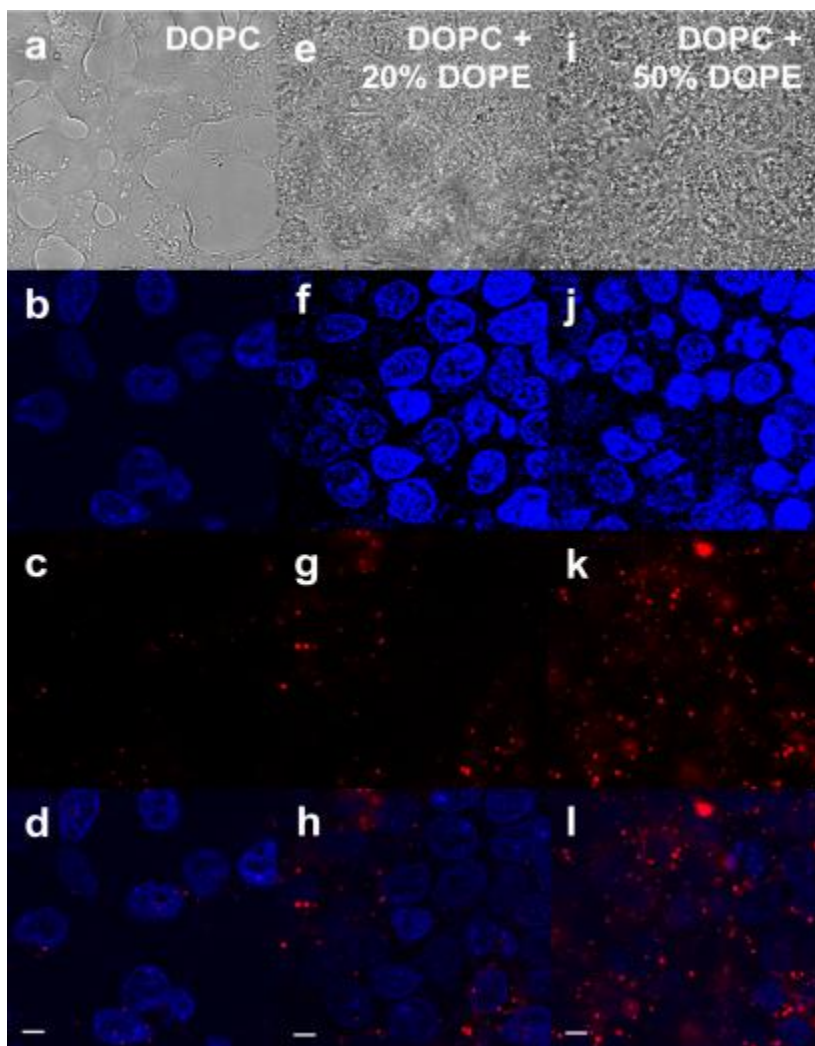


Fig. S5: DOPE improves uptake of DOPC liposomes. To a lesser extent than dpA3 nanofibers, the addition of DOPE improves the transfer of DiI from DOPC liposomes to cells. Panels (a) (e) and (i) are DIC images of cells in field of view. Panels (b) (f) and (j) show DAPI labeled nuclei of the imaged cells. Panels (c) (g) and (k) are images obtained from the red channel for DiI. Panels (d) (h) and (l) are overlays of DAPI and DiI channel. Panels (a) to (d) show minimal uptake of 0.2% DiI labeled DOPC liposomes. Addition on DOPE increased uptake of DOPC liposomes (e) to (l). The Concentration of lipids were kept at $\sim 17 \mu\text{M}$ in all three experiments. Scale bar represents $5 \mu\text{m}$.

Supplementary Figure 6 (Fig. S6)

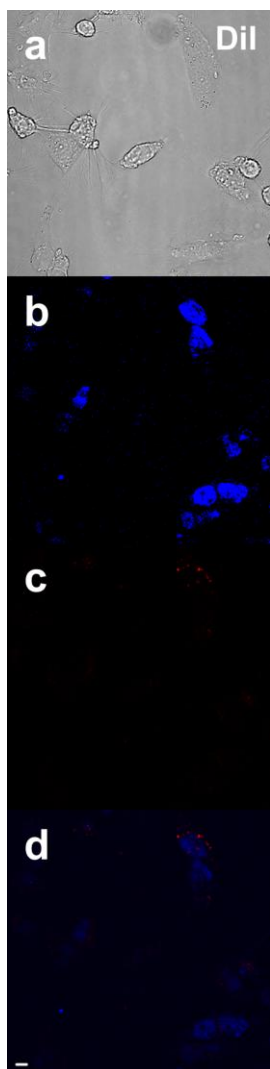


Fig. S6: DiI is not internalized by HeLa cells. Equivalent quantities of DiI were dried down and hydrated. Due to its hydrophobicity DiI was not very soluble in diH₂O. The solution is collected and undissolved DiI spun down. The supernatant was then added to HeLa cells. Panel (a) is DIC image of cells in field of view. Panel (b) shows DAPI labeled nuclei of the imaged cells. Panel (c) is the image obtained from the red channel for DiI. Panel (d) is the overlay of DAPI and DiI channel. Panels (a) to (d) show no staining of cell membranes by DiI. This suggests that DiI is a good marker for lipid based nanoparticles and that a delivery vehicle is required for DiI delivery to the cell. Scale bar represents 5 μ m.